PLEA 2018 HONG KONG
Smart and Healthy within the 2-degree Limit

Potential Wind Power Utilization in Diverging Passages Between Two High-Rise Buildings:

Using "Venturi effect" on the Windward Side

YU-HSUAN JUAN[1], CHIH-YUNG WEN[1], AN-SHIK YANG[2], HAMID MONTAZERI[3,4], BERT BLOCKEN [3,4]

[1]The Hong Kong Polytechnic University, Hong Kong
[2]National Taipei University of Technology, Taiwan
[3]Eindhoven University of Technology, Netherlands
[4]KU Leuven, Leuven, Belgium

ABSTRACT: The objective of this study is to investigate the urban wind power potential from the proper arrangement of high-rise buildings in a complex and dense urban environment. There is great prospective in the formulation of the building design at early stages to maximize wind power production in dense urban areas. We employed the 3D steady Reynolds-averaged Navier-Stokes computational fluid dynamics (CFD) simulations to investigate the impact of the arrangement of high-rise buildings on the wind energy potential . Two arrays of high-rise buildings with height = 90 m and aspect ratio (height/width) of 4.5 is studied, which focuses on different distances between the side façades of the upstream buildings, ranging from 3 to 21 m. The findings of the study support the high-rise buildings design with respect to integrated urban wind energy harvesting and the concept of sustainable urban development.
KEYWORDS: Urban Wind Energy, High-rise Building, Wall Effect, Urban Design

1. INTRODUCTION

Recently, the wind power has become one of the most accessible resources among renewable energy alternatives in high-rise and high-density urban areas. Because of the disturbed flows around buildings, the structures can accelerate wind speeds to increase the wind power density as compared to the case for the airflow over open areas. Incorporating wind turbines into the building design are stepping into our lives. Nonetheless, the high-rise buildings are subject to the significant interaction with the wind power resource. The urban wind environment is substantially affected by the presence of buildings with the wind velocities increased especially on the roof, edges and vertical windward walls of buildings [1]. Lu and Ip explored the feasibility and enhancement methods of wind power utilization around high-rise buildings of Hong Kong [2]. Khayrullina et al. conducted CFD simulations to examine the wind conditions in passages between parallel buildings for assessing wind energy potential [3]. Chaudhry et al. studied the influence of building morphology, including triangular, square and circular cross-sections, on the efficiency of building-integrated wind turbines (BIWT) [4]. Balduzzi et al. evaluated a wind turbine for installation on the roof of a selected building with certain roof geometric features [5]. However, the above research lacked to consider the wind flows behind high-rise buildings.

In high-density urban areas, the high-rise buildings may result in an insufficiency of air ventilation, since the airflow is blocked by structures along the coastal line. The number of high-rise buildings has continually increased in recent years. Those buildings can impede the flowing of fresh air, which is vital for ventilation and pollutant dispersal in street canyons [6]. Clusters of buildings can obstruct air flow into the street pass ways and thereby reduce air flow velocity.

We devise two different scenarios. Scenario A consists of a 1×2 array of high-rise buildings, while Scenario B a 2×2 array of buildings. Essentially, we investigate the building orientations of θ = 0 and 45° in the passages, which varied the distance between upstream buildings. Recent studies showed that the "Venturi effect" arrangement coupled with the building diverging passages can be a better choice to promote ventilation at the pedestrian level [1, 6-10]. While several studies have been performed to investigate the urban wind energy potential, the impact of the arrangement of high-rise buildings has not yet investigated in detail. In this paper, therefore, the impact of the arrangement of high-rise buildings on the wind energy potential is investigated. The findings of the study support the design of high-rise buildings with respect to integrated wind energy harvesting especially. In addition, the studied results can be of interest to urban planners, designers and builders. The building dimensions, and the vertical inlet profiles of velocity is based on a dense urban area in the central region of Hong Kong, to address the schemes on the development of wind power in local urban areas for maximizing wind energy utilization.

2. METHODS

2.1 Building geometries for different scenarios

This study investigates the urban wind power potential using the concentration effect between an arrangement of a representative parallel high-rise building array (90 m × 20 m × 20 m with a distance of 3 m) as Scenario A, simplified from a realistic urban pattern of Central, Hong Kong, as displayed in Fig. 1.

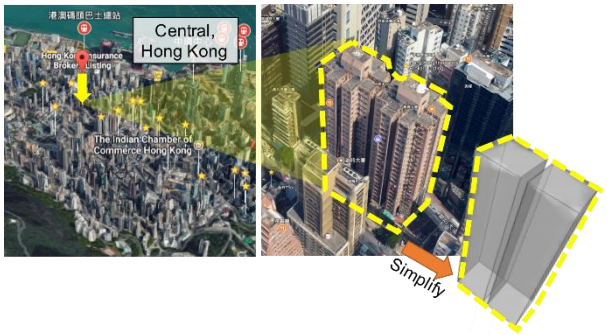

Figure 1: Two parallel building blocks simplified from two high-rise buildings in Central, Hong Kong

Two scenarios are considered to investigate the wind flows over high-rise buildings, with varied geometrical situations in terms of building layouts and distances, as listed in Table 1. To study the concentration effect of two parallel high-rise buildings without placing the barrier of buildings on the windward side in Scenario A, Case 0 was simulated with the distance of 3 m, as depicted in Fig. 2. In contrast, Scenario B considered varied canyon layouts at the distances from upstream buildings of D= 3m, 6m, 9m, 12m, 15m, 18m and 21m. Besides, the building orientation was turned 135° of the diverging passage on the windward side (detailed in Ref. 8) to compare the wind flow field with that of Scenario A, which is expected to be an appropriate arrangement for forming the "Venturi effect" shape, as depicted in Fig. 2. From the predictions, this study then inspects the effectiveness of the concentration effect of high-rise buildings to fully utilize urban wind energy.

Table 1: Geometries of Scenario A and B

Scenario	Case	Upstream buildings distance
A	0	-
B	1	3 m
	2	6 m
	3	9 m
	4	12 m
	5	15 m
	6	18 m
	7	21 m

2.2 CFD validation study

The simulations are based on validation with the wind tunnel experiment by Stathopoulos and Storms [11] for a scale of 1/400 in the boundary layer wind tunnel of the Centre for Building Studies (CBS) . Two buildings with dimensions of 20 m× 20 m× 40 m ($H \times D \times L$ in a full scale) with a 6-m passage distance in the wind-tunnel experiments are considered, while the wind flow direction was parallel to the passage center line. In this section, we first reproduced the geometric details of the wind tunnel to the simulation model, implementing a high grid resolution near the ground of the computational domain to comply with the requirements of near-ground flows.

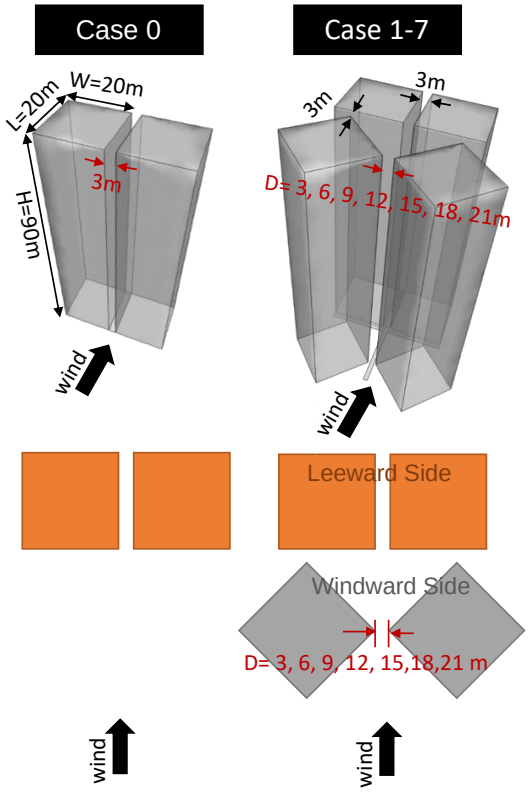

Figure 2: Geometries of Scenario A and B

The neutral atmospheric boundary layer (*ABL*) was described using a power-law form with exponent 0.15. The reference wind speed U_{ref} was 5.9 m/s at 2m height of the pedestrian level (in full scale), and the turbulence intensity of the incident flow ranged from 20% at 2m height to 5% at a gradient height of 360 m. The profiles of the mean wind speed and turbulence intensity at the inlet were prescribed employing the incident profiles from the wind-tunnel measurements. The computational domain and grids are based on the CFD guidelines [12, 13]. The distances from the buildings to the top, inlet, outlet and lateral boundaries are 5H, 5H, 15H and 5H (with the term H representing the building height), respectively. The wall roughness was expressed by an

equivalent sand-grain roughness K_S in the wall functions, setting as 30 times of z_0 [14]. We only used the hexahedral grids with a grid expansion ratio of 1.1 and the least grid size of 0.005 m. The total number of cells was 2,246,100. The grid is generated based on a grid-sensitivity analysis, where coarsening and refining is performed with an overall linear factor 2. The commercial CFD software ANSYS/Fluent® 18.0 is used to solve the three-dimensional Reynolds-averaged Navier–Stokes (RANS) equations in combination withthe realizable *k–ε* model [15]. The SIMPLE algorithm is used to couple the velocity and pressure [16-17]. Second-order discretization schemes are used for both the convection terms and the viscous diffusion terms.

The validation results reveal that the calculated streamwise velocity and turbulent kinetic energy profiles from the standard and realizable *k-ε* models are relatively more accurate than those from the RNG and SST *k-ω* models. Moreover, the predictions of the Z velocity profiles by the standard and RNG *k-ε* models agreed reasonably well with the measurement data. The prediction capability of the standard *k-ε* turbulence model shows the best agreement between the CFD calculations and the wind tunnel measurements.

2.3 Computational approach

At the inlet of the domain neutral ABL inflow profiles of mean velocity (U_{ABL}), turbulent kinetic energy (k), and turbulence dissipation rate profiles (ε) are imposed [14].

$$U_{ABL} = \frac{u^*_{ABL}}{K} \ln\left(\frac{z + z_0}{z_0}\right) \quad (1)$$

$$k = \frac{(u^*_{ABL})^2}{\sqrt{C_u}} \quad (2)$$

$$\varepsilon = \frac{(u^*_{ABL})^3}{K(z + z_0)} \quad (3)$$

$$u^*_{ABL} = \frac{KU_h}{\ln\left(\frac{h + z_0}{z_0}\right)} \quad (4)$$

where z_0 and κ are the aerodynamic roughness and the von Karman's constant (≈ 0.4), respectively. The ABL friction velocity u^*_{ABL} is computed from a specified velocity U_h at a reference height h. The mean inlet velocity at the height of z (U_{ABL}), was obtained via Eq. (1) to generate a velocity profile in the ABL with the turbulence kinetic energy k and dissipation rate ε computed by Eqs (2) and (3), respectively. From the data of a local meteorological station, the annual mean speed of 4.4 m/s at 10 m was used to calculate the ABL velocity. In essence, roughness will increase the drag for the cross-flow over the surface, causing the case that the logarithmic law for velocity profile, being the basis of the standard wall function, is not valid in the roughness case. This study modeled the real obstruction effect on the wind flow in terms of equivalent roughness by the roughness wall functions to replace the obstacles applied to the bottom plane of the domain [6,14].

This case specified the aerodynamic roughness z_0 as 0.7 m to replicate the terrain of high-rise buildings in accordance with the updated Davenport roughness classification. In addition, we set the constant static pressure boundary condition at the outlet. The symmetric conditions were implemented by prescribing the zero normal component of velocity and zero normal derivatives for all flow variables at the top and lateral boundaries. Zero-gauge static pressure was set at the outlet. Convergence is assumed to obtain when all the scaled residuals levelled off and reached a minimum of 10^{-5} for continuity and turbulence dissipation rate, 10^{-6} for velocities and turbulent kinetic energy.

Table 2: Boundary conditions of CFD simulations

Boundary	***Type***
Inlet	Velocity-inlet
Outlet	Pressure-outlet
Top	Symmetry
Lateral	Symmetry
Building	Wall
Ground	Wall

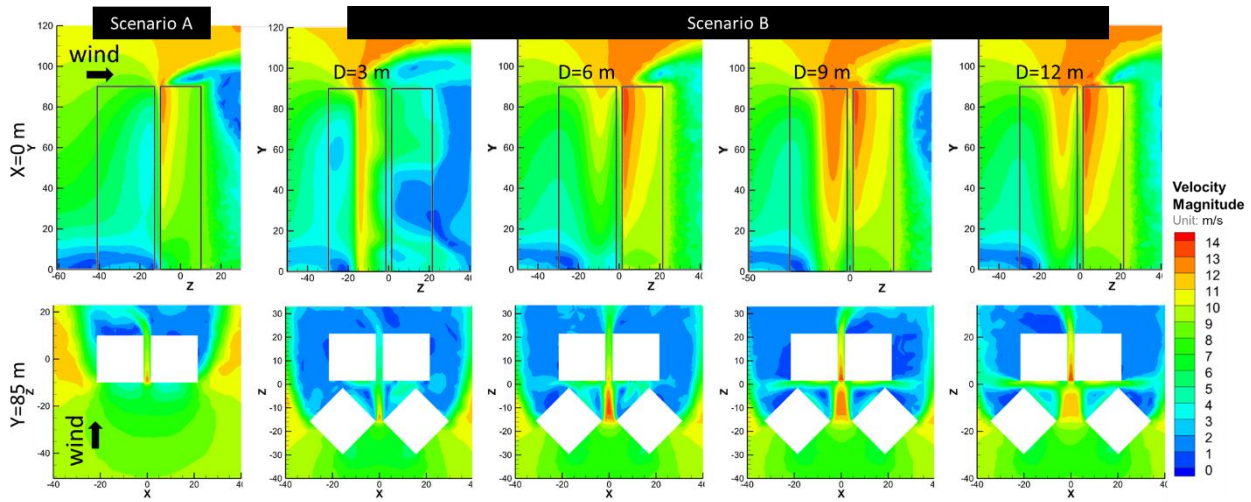

Figure 3: Predicted velocity magnitude contours in vertical sections at x= 0m and y= 85m

3. RESULTS

3.1 Scenario A

CFD simulations considered Case 0 as the baseline case with no obstacle of upstream high-rise buildings on the windward side in a high-rise building 1×2 array. We analysed the conditions at a building distance of 3 m, as displayed in Figs. 3 and 4. Figure 3 illustrates the wind speed distributions in vertical sections at x= 0m and y= 85m for Scenario A and B. It can be observed that the wind speed in the vertical channel of two buildings augmented sharply from the inlet boundary, arrived at the greatest value at the narrowest point of two buildings and then decreases. For Scenario A in Fig. 3, the maximum wind velocity reaches approximately 12.3 m/s near the leading edge between buildings. In this study, the wind power density is used to evaluate the wind power potential, as the following Equation (5):

$$P = 0.593\rho v^3, \qquad (5)$$

where P - power density (W/m^3);
ρ- air density (kg/m^3);
v - air speed (m/s).

Figure 4 shows the predicted power density contours in three different sections at x= 0m, y= 85m and y=93 m for Scenario A. As a result, the associated power density can be up to 1200 W/m^2. In Scenario B, the wind energy over the roof generally grows with the increasing distance between upstream buildings because of the concentration effect of downstream buildings.

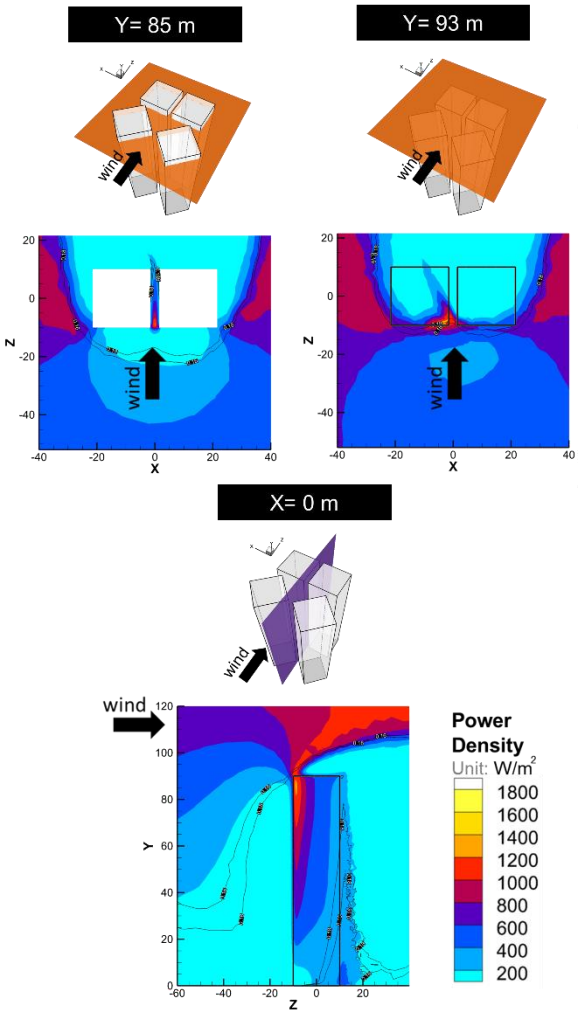

Figure 4: Predicted power density contours in three different sections at x= 0m, y= 85m and y=93 m for Scenario A

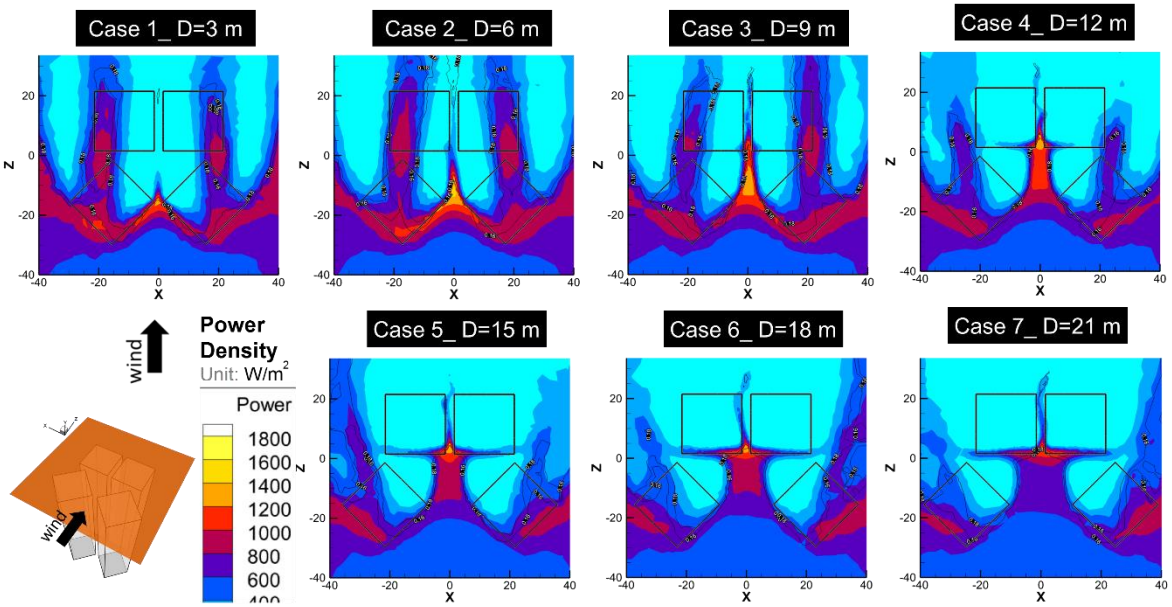

Figure 5: Predicted power density contours in horizontal sections of Y= 93 m above the roof

3.2 Scenario B

Reducing the obstacle behind high-rise buildings, Scenario B further incorporated the Venturi effect in the passages configuration into upstream buildings with the building orientation arranged 45° of passage. To examine the influences of upstream buildings on the urban wind power production, different distances are considered D= 3m, 6m, 9m, 12m, 15m, 18m and 21m (i.e. Case 1-7) to make a comparison of the energy yields from the above cases with that from Case 0 in Scenario A without upstream high-rise buildings. The CFD results in Fig. 3 reveal higher wind speeds at the widest distance between upstream high-rise buildings. Thus, the predictions indicates that the wind speeds of D = 9m and 12m over the upstream buildings are higher than those of D = 3m and 6m. The situation without blocking of upstream buildings observed smooth flow of the approaching wind through the street canyon, leading to higher velocities in the downstream area. Figure 5 shows the predicted power density distributions above the roof in horizontal sections of Y= 93 m. It can be seen that wind energy harvesting over the roof generally raises by the increase of the distance between upstream high-rise buildings due to the concentration effect of downstream high-rise buildings. The results in Figs. 3 and 5 indicated that the "Venturi effect" configuration on the windward side can significantly increase the wind velocity and power generation.

Figure 6 illustrates the predicted power density profiles against height at the point (X, Z)= (0 m, 2.8 m) between the leading edge of downstream buildings for all cases in Scenario A and B. We notice that the wind power densities in Scenario A were greater than those for the cases at D= 3m and 6m. Moreover, the power densities for the incidents at D= 9m, 12m, 15m, 18m, and 21m appear to be productive in Scenario B. We identified the site between downstream buildings passage under the top roof as the most appropriate location to install micro wind turbines for operation and maintenance of wind power management. More precisely, a further increase in width for the best case at D=12 m provided less than 1% variation in the wind velocity and power generation.

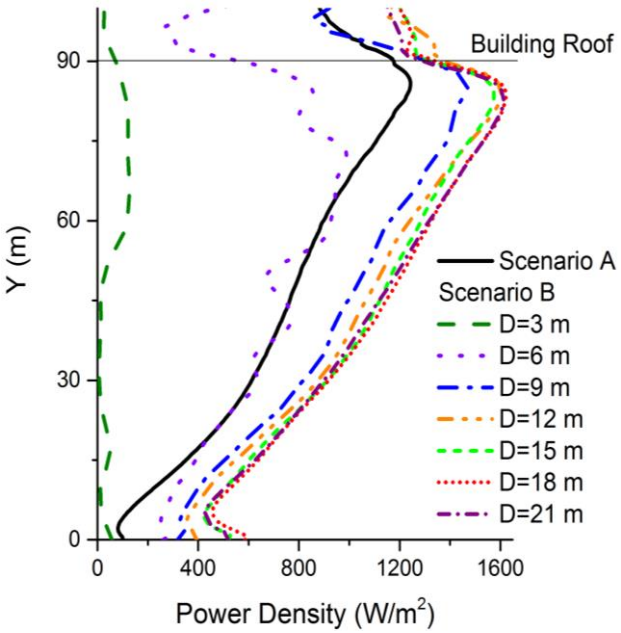

Figure 6. Predicted power density profiles against height at varied distances from upstream buildings in Scenario A and B

4. DISCUSSION

The limitations of this study are listed as follows and will be addressed in future work.

(1) This study is conducted based on one wind direction of wind velocity.
(2) The focus in this paper is on wind speed and power density for assessing the potential wind power utilization. Future work should apply and compare different indices like turbulence intensity, to assess urban wind power utilization.

In spite of these limitations, the issue of concern here is on the appropriateness of using the variations upstream building layout to check the effectiveness of the concentration effect of high-rise buildings for fully utilization of the urban wind energy. It provides practical implications for urban planners, designers and policymakers to adopt the upstream buildings configurations with the optimization of the street geometry and urban morphology for enhancing city breathability and increasing urban wind power usage.

5. CONCLUSION

From the aforementioned studies examining the influences of upstream and downstream buildings on urban wind power exploitation, the results led to the following conclusions.

(1) The 'Venturi effect' on the windward side can noticeably increase the wind velocity and power generation with respect to the increasing distance between upstream buildings.
(2) The diverging inlet in Scenario B produced greater concentration outcome of the wind at a height under the roof than that above the roof.
(3) The best case for the model with D= 12 m showed that a further increase in width provided less than 1% discrepancy in the wind velocity and power generation.

ACKNOWLEDGEMENTS

This study represents part of the results obtained under the support of Environment and Conservation Fund, Hong Kong, ECF 51/2016 and Ministry of Science and Technology, Taiwan, ROC (Contract No. MOST105-2221-E-027-098 and 107-2917-I-027 -001).

REFERENCES

1. Yang, A.S., Su, Y.M., Wen, C.Y., Juan, Y.H., Wang, W.S. and Cheng, C.H., (2016). Estimation of wind power generation in dense urban area. *Applied Energy*, 171:p. 213-30.
2. Lu, L., & Ip, K. Y. (2009). Investigation on the feasibility and enhancement methods of wind power utilization in high-rise buildings of Hong kong. Renewable and Sustainable Energy Reviews, 13(2), 450-461.
3. Khayrullina, A., van Hooff, T. v., & Blocken, B. (2013). A study on the wind energy potential in passages between parallel buildings. Paper presented at the Proceedings of the 6th European-African Conference on Wind Engineering (EACWE), Cambridge, UK.
4. Chaudhry, H. N., Calautit, J. K., & Hughes, B. R. (2014). The influence of structural morphology on the efficiency of building integrated wind turbines (biwt). AIMS Energy, 2(3), 219-236
5. Balduzzi, F., Bianchini, A., & Ferrari, L. (2012). Microeolic turbines in the built environment: Influence of the installation site on the potential energy yield. Renewable Energy, 45, 163-174.
6. Juan, Y.H., Yang, A.S., Wen, C.Y., Lee, Y.T., Wang, P.C. (2017). Optimization procedures for enhancement of city breathability using arcade design in a realistic high-rise urban area. BUILD ENVIRON, 121, p.247-261.
7. Blocken, B., Moonen, P., F.ASCE, T. S., and Carmeliet, J., (2008). Numerical study on the existence of the venturi effect in passages between perpendicular buildings. *Journal of Engineering Mechanics*, 134(12):p. 1021-1028.
8. Li, B., Luo, Z., Sandberg, M., and Liu, J., (2015), Revisiting the 'venturi effect' in passage ventilation between two non-parallel buildings. *Building and Environment,* 94, p. 714-722.
9. Montazeri, H., Blocken, B. (2013). CFD simulation of wind-induced pressure coefficients on buildings with and without balconies: Validation and sensitivity analysis. *Building and Environment,* 60, p.137-149.
10. Rezaeiha, A., Montazeri, H., Blocken, B. (2018). Towards accurate CFD simulations of vertical axis wind turbines at different tip speed ratios and solidities: Guidelines for azimuthal increment, domain size and convergence. *Energy Conversion and Management*, 156, p.301-316.
11. Stathopoulos, T., Storms, R. (1986). Wind environmental conditions in passages between buildings. *Journal of Wind Engineering and Industrial Aerodynamic*s, 24, p.19-31.
12. Franke, J., Baklanov, A. (2007). Best practice guideline for the CFD simulation of flows in the urban environment COST action 732 Quality assurance and improvement of microscale meteorological models. Hamburg: Meteorological Inst.
13. Casey, M., Wintergerste, T. (2000). ERCOFTAC best practice guidelines : ERCOFTAC special interest group on "quality and trust in industrial CFD". London: ERCOFTAC.
14. Blocken, B., Stathopoulos, T., Carmeliet, J. (2007). CFD simulation of the atmospheric boundary layer: wall function problems. *Atmospheric Environment*, 41, p.238-52.
15. Hang, J., Sandberg, M., Li, Y. (2009). Effect of urban morphology on wind condition in idealized city models. Atmospheric Environment, 43,p.869-78.
16. Hang, J., Luo, Z., Sandberg, M., Gong, J. (2013). Natural ventilation assessment in typical open and semi-open urban environments under various wind directions. *Building and Environment*, 70,p.318-33.
17. ANSYS Inc. (2013). A. ANSYS Fluent Theory Guide for Release 15.0. U.S.A.